ACCEPTED BY THE ASTRONOMICAL JOURNAL
Preprint typeset using LaTeX style emulateapj v. 11/10/09

RESOLVED SPECTROSCOPY OF M DWARF/L DWARF BINARIES. IV. DISCOVERY OF AN M9 + L6 BINARY SEPARATED BY OVER 100 AU

SAURAV DHITAL [1], ADAM J. BURGASSER [2,5], DAGNY L. LOOPER [3,5], KEIVAN G. STASSUN [1,4]

(Accepted October 6, 2010)
Submitted: August 9, 2010

ABSTRACT

We report the discovery of a faint L6±1 companion to the previously known M9 dwarf, 2MASS J01303563−4445411, based on our near-infrared imaging and spectroscopic observations with the 3m Infrared Telescope Facility SpeX imager/spectrometer. The visual binary is separated by 3.″28±0.″05 on the sky at a spectrophotometric distance of 40±14 pc. The projected physical separation is 130±50 AU, making it one of the widest VLM field multiples containing a brown dwarf companion. 2MASS J0130−4445 is only one of ten wide VLM pairs and only one of six in the field. The secondary is considerably fainter ($\Delta K \approx$ 2.35 mag) and redder ($\Delta\ (J - K_s) \approx 0.81$ dex), consistent with component near-infrared types of M9.0±0.5 and L6±1 based on our resolved spectroscopy. The component types suggest a secondary mass below the hydrogen-burning limit and an age-dependent mass ratio of 0.6–0.9. The system's space motion and spectroscopic indicators suggest an age of 2–4 Gyr while the model-dependent masses and binding energies suggest that this system is unlikely to have formed via dynamical ejection. The age, composition, and separation of the 2MASS J01303563−4445411 system make it useful for tests of VLM formation theories and of condensate cloud formation in L dwarfs.

Subject headings: binaries: visual — stars: individual (2MASS J01303563−4445411) — stars: low mass, brown dwarfs

1. INTRODUCTION

The processes by which very low-mass (VLM; M $\lesssim$0.1 $M_\odot$, Burgasser et al. 2007c) stars and brown dwarfs (BD) form, and whether these processes are similar to those of higher-mass stars, is an open question. The VLMs/BDs exhibit significant differences in the distribution of binary/multiple systems when compared to their more massive brethren. The resolved binary fraction of ∼20–30% in VLMs/BDs (Basri & Reiners 2006; Joergens 2008) is significantly lower than in F and G dwarfs (∼60%; Duquennoy & Mayor 1991) and modestly lower than M dwarfs (∼27–42%; Fischer & Marcy 1992; Reid & Gizis 1997). The typical orbital separation of ∼4–5 AU in VLMs/BDs is much smaller compared to ∼30 AU for F, G, and M dwarf binaries (Duquennoy & Mayor 1991; Fischer & Marcy 1992). In addition, while stellar binaries are known to have separations in excess of ∼1 pc (e.g., Lépine & Bongiorno 2007; Dhital et al. 2010), no VLM system has a separation greater than 6700 AU. Indeed, only 15 of the known 99 VLM systems have projected physical separations larger than 20 AU and only nine systems are wider than 100 AU[6]. Energetically, the VLM binaries seem to stand apart as well: based on empirical data, Close et al. (2003) suggested minimum binding energies of $10^{42.5}$ erg for field VLM systems, ∼300 times higher than the 10^{40} erg limit for stellar binary systems. Lastly, most VLM binaries are close to equal-mass. All of these differences indicate that the same formation process(es) may not be responsible for the two populations.

It is now generally believed that most stars form in multiple systems via fragmentation of the protostellar cloud, with single stars being the result of decay of unstable multiples (e.g., Kroupa 1995). The most favored process is gravoturbulence where the fragmentation is the result of a combination of turbulent gas flows and gravity. Hydrodynamical simulations have shown that when turbulent gas flows in protostellar clouds collide, they form clumps that are gravitationally unstable and, hence, collapse forming multiple stellar embryos (e.g., Caselli et al. 2002; Goodwin et al. 2004a,b; Bate 2009). Within a few freefall times, most of these embryos are ejected due to mutual dynamical interactions, preferentially the ones with lower masses.

To then explain the observed distributions of VLM binaries separations, two explanations have been proffered. The first so-called "ejection hypothesis" suggests that most VLM binaries, unlike the more-massive stellar systems, are the result of the ejected embryos (Reipurth & Clarke 2001). The wider systems get disrupted, explaining the overall rarity of VLM and BD binaries. The second is preferential accretion within the first 0.1 Myr (∼1 freefall time), making VLM systems tighter and more equal-mass. As a result, even VLM distributions that initially may have looked similar to that of higher mass stars are transformed and look like the observed VLM distributions (Bate 2009). However, neither hypothesis explains why ∼10% of observed VLM binaries are wider than 100 AU. Two other theories on VLM/BD formation, disk fragmentation (e.g., Watkins et al. 1998a,b) and photoablation (Whitworth & Zinnecker 2004), require massive stars to trigger the process and cannot explain the existence of VLM bi-

[1] Department of Physics & Astronomy, Vanderbilt University, Nashville, TN, 37235, USA; saurav.dhital@vanderbilt.edu
[2] Center of Astrophysics and Space Sciences, Department of Physics, University of California, San Diego, CA 92093, USA
[3] Institute for Astronomy, University of Hawaii, 2680 Woodlawn Drive, Honolulu, HI 96822, USA
[4] Department of Physics, Fisk University, 1000 17th Avenue North, Nashville, TN 37208, USA
[5] Visiting Astronomer at the Infrared Telescope Facility, which is operated by the University of Hawaii under Cooperative Agreement no. NCC 5-538 with the National Aeronautics and Space Administration, Science Mission Directorate, Planetary Astronomy Program.
[6] VLM Binaries Archive (`http://vlmbinaries.org/`) and references therein.

naries in the field. To resolve the differences between observational and numerical results and to distinguish between the various formation scenarios, a larger sample of VLM binaries—especially very wide systems that are most susceptible to dynamical effects—is needed.

In this paper, we report the discovery of a wide VLM binary 2MASS J01303563−4445411 (hereafter 2MASS J0130−4445) separated by 130 AU, 3.″3. The brighter primary component of 2MASS J0130−4445 was identified by Reid et al. (2008) in the Two Micron All Sky Survey (2MASS; Skrutskie et al. 2006) and classified as an M9 dwarf on the Kirkpatrick et al. (1999) red optical scheme, indicating a spectrophotometric distance of 33.1±2.2 pc. Neither Hα nor Li I, activity and age indicators, respectively, were evident in the optical spectrum. The primary has a proper motion of (120±14, -25±20) mas yr^{-1}and a tangential velocity of 19±3 km s^{-1}(Faherty et al. 2009). The system is unresolved in 2MASS, and there have been no reports of a faint companion to this source in either optical survey data or follow-up observations (Reid et al. 2008; Faherty et al. 2009).

In our own follow-up observations of 2MASS J0130−4445, we have identified a well-separated, faint L dwarf companion, indicating that this is a wide VLM binary system with a probable BD component. In Sections 2 and 3, we describe our imaging and spectroscopic observations, respectively, and discuss the properties of the components of the resolved binary system. We discuss the physical association, mass, and age of the binary 2MASS J0130−4445AB in Section 4 and its implications on VLM formation and evolution scenarios in Section 5. The conclusions are presented in Section 6.

2. NEAR-INFRARED IMAGING

2.1. *Observations and Data Reduction*

2MASS J0130−4445 was imaged with the 3m NASA Infrared Telescope Facility (IRTF) SpeX spectrograph (Rayner et al. 2003) on December 7, 2009 (UT), as part of a program to identify unresolved M/L dwarf plus T dwarf spectral binaries (e.g., Burgasser et al. 2008). Conditions were clear but with poor seeing, 1.″2 at K-band, due in part to the large airmass of the observation (2.34–2.37). These images revealed a faint point source due east of the primary target at a separation of roughly 3″. Four dithered exposures were obtained of the pair in each of the MKO[7] J, H, and K filters, with individual exposure times of 45s, 30s, and 30s, respectively. The field rotator was aligned at a position angle of 0°; i.e., north up and east to the left.

Imaging data were reduced in a standard manner using custom IDL routines. Raw images were mirror-flipped about the y-axis to reproduce the sky orientation and pair-wise subtracted to remove sky contributions. The difference images were divided by normalized flat field frames, constructed by median-combining the imaging data for each filter after masking out the sources. Subsections of each image, 10″ (83 pixels) on a side and centered on the target source, were extracted from these calibrated frames. A final image for each filter/target pair (Figure 1) was produced by averaging the registered subframes together, rejecting 5σ pixel outliers. The two sources of 2MASS J0130−4445 are well resolved along a nearly east-west axis. The brighter western component is hereafter referred to as 2MASS J0130−4445A and the eastern component as 2MASS J0130−4445B.

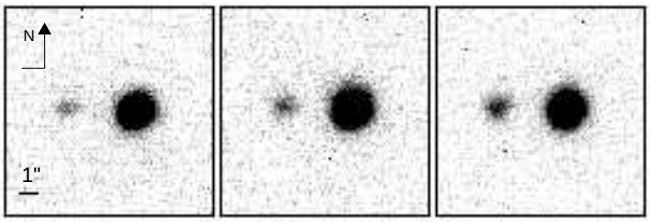

Figure 1. Combined SpeX images of 2MASS J0130−4445AB in the J-, H- and K-bands (left to right), showing the 10″×10″ (83×83 pixel) region around both sources. Images are aligned with north up and east to the left.

Table 1
Results of PSF Fitting

Parameter	Value
$\Delta\alpha\cos\delta$ (″)[a]	3.28±0.05
$\Delta\delta$ (″)[a]	0.15±0.06
Apparent Separation (″)	3.28±0.05
Position Angle (°)[a]	87.3±0.9
ΔJ (mag)	3.11±0.06
ΔH (mag)	2.68±0.11
ΔK (mag)	2.34±0.04

[a] Measured from the brighter primary to the fainter secondary.

2.2. *Analysis*

Component magnitudes and the angular separation of the 2MASS J0130−4445 pair were determined through point spread function (PSF) fits to the reduced imaging data, following the prescription described in McElwain & Burgasser (2006). The PSF models were derived from Gaussian fits to the primary component in the individual subimage frames. For each filter, four distinct PSF models were produced, each of which were fit to the individual images, resulting in a total of 16 independent measures of the relative component magnitudes and 48 independent measures of the separation and orientation of the pair, in each of the JHK filters. However, as the secondary was undetected in one of the four J-band images, four measures of the relative J-band flux and separation were discarded before computing mean values and standard deviations. Separation measurements were converted from pixels to arcseconds assuming a plate scale of 0.″120±0.″002 pixel^{-1} (J. Rayner, 2005, private communication) and no distortion. The position angle (set at 0°) was assumed to be accurate to within 0.°25 (ibid.).

Results are listed in Table 1. The angular separation of the pair was measured to be 3.″282±0.″047 at a position angle of 87.°3±0.°9; i.e., along an east-west line. The secondary is both considerably fainter and significantly redder than the primary. We derived relative magnitudes of $\Delta J = 3.11\pm0.06$ and $\Delta K = 2.34\pm0.04$. Using the combined-light 2MASS photometry for the system[8], this translates into $J - K_s$ colors of 1.13±0.04 and 1.94±0.08 for the primary and secondary, respectively.

3. NEAR-INFRARED SPECTROSCOPY

[7] Mauna Kea Observatory filter system; see Tokunaga et al. (2002) and Simons & Tokunaga (2002).

[8] We included small corrections to the relative magnitudes in converting from the MKO to 2MASS photometric systems: 0.009, -0.006, and -0.003 mag in the J, H, and K/K_s bands, respectively, calculated directly from the spectral data.

3.1. *Observations and Data Reduction*

The two components of 2MASS J0130−4445 were observed on separate nights with the prism-dispersed mode of SpeX, the primary on December 7, 2009 (the same night as the imaging observations) and the secondary on December 28, 2009 (UT). Conditions on the latter night were clear with a stable seeing of 0.″6 at K-band. The SpeX prism mode provides 0.75–2.5 μm continuous spectroscopy with resolution $\lambda/\Delta\lambda \approx 120$ for the 0.″5 slit employed (dispersion across the chip is 20–30 Å pixel^{-1}). Both components were observed separately, with the slit oriented north-south, roughly aligned with the parallactic angle and perpendicular to the separation axis. For the primary, eight exposures of 90s each were obtained at an average airmass of 2.33, while guiding on spillover light from the slit. For the secondary, eight exposures of 150s each were obtained at an average airmass of 2.34, while guiding on the primary off-slit. For both sources, the A0 V star HD 8977 was observed immediately before the target for telluric and flux calibration while the quartz and Ar arc lamps were observed for flat field and wavelength calibration, respectively. Data were reduced using the SpeXtool package, version 3.4 (Vacca et al. 2003; Cushing et al. 2004) using standard settings; see Burgasser et al. (2007b) for details.

3.2. *Analysis*

Figure 2 shows the spectra of the two components of 2MASS J0130−4445AB; signal-to-noise at the JHK flux peaks was 100–150 and 25–35 for the A and B components, respectively. Both spectra show the characteristic near-infrared (NIR) features of late-type M and L dwarfs (e.g., Reid et al. 2001; McLean et al. 2003; Cushing et al. 2005): steep red optical slopes (0.8–1.0 μm) from the pressure broadened wing of the 0.77 μm K I doublet; molecular absorption bands arising from H_2O (1.4 and 1.9 μm), CO (2.3 μm), and FeH (0.99 μm); and an overall red spectral energy distribution (SED), consistent with the photometric colors. 2MASS J0130−4445A also exhibits additional absorption features in the 0.8–1.2 μm region arising from TiO, VO, FeH, and unresolved K I and Na I lines, all typical for a late-type M dwarf. The corresponding region in the spectrum of 2MASS J0130−4445B is considerably smoother, albeit more noisy, suggesting that many of these gaseous species have condensed out (e.g., Tsuji et al. 1998; Ackerman & Marley 2001). The appearance of weak H_2O absorption at 1.15 μm and the very red SED of the NIR spectrum all indicate that 2MASS J0130−4445B is a mid- to late-type L dwarf with relatively thick condensate clouds at the photosphere.

To determine spectral types we compared our NIR spectra of 2MASS J0130−4445AB with 463 spectra of 439 M7 or later dwarfs from the SpeX Prism Spectral Libraries[9]. All templates wre chosen to have median S/N > 10 and could not be binaries, giants, subdwarfs, or spectral classifications that were peculiar or uncertain. Best matches were determined by finding the minimum χ^2 deviation between component spectra and templates in the 0.95–1.35, 1.45–1.80, and 2.00–2.35 μm regions (i.e., avoiding telluric bands), following the procedure of Cushing et al. (2008) with no pixel weighting. The two best matching templates to both components of 2MASS J0130−4445AB are shown in Figure 3. For 2MASS J0130−4445A, these are the optically classified

[9] `http://browndwarfs.org/spexprism/`

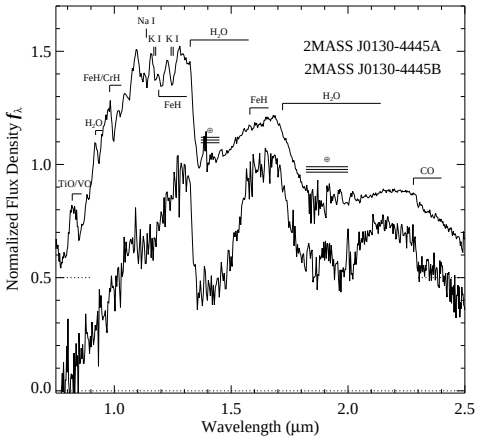

Figure 2. NIR spectra of 2MASS J0130−4445A (top) and 2MASS J0130−4445B (bottom) obtained with IRTF/SpeX. Data are normalized at the peak of each spectra, and the spectrum for 2MASS J0130−4445A is vertically offset by 0.5 dex for clarity (dotted lines). NIR spectral features are labeled.

M8 dwarf 2MASS J05173729−3348593 (Cruz et al. 2003) and L0 dwarf DENIS–P J0652197−253450 (Phan-Bao et al. 2008); for 2MASS J0130−4445B these are the optically classified L5 dwarf 2MASSW J1326201−272937 (Gizis 2002) and L7 dwarf 2MASS J03185403−3421292 (Kirkpatrick et al. 2008). Note that despite the differences in optical type, these spectra provide equivalently good fits—the two fits were different only by 1.7σ for the primary and 1.1σ for the secondary based on the F-test which gauges whether two different fits to data are significantly distinct based on the ratio of χ^2 values and degrees of freedom (Burgasser et al. 2010)—to the components of 2MASS J0130−4445AB, a reflection of the discrepancies between optical and NIR spectral morphologies for late-type M and L dwarfs (e.g., Geballe et al. 2002; Kirkpatrick 2005). A χ^2 weighted mean of all the SpeX templates (e.g., Burgasser et al. 2010) indicates component types of M9.0±0.5 for 2MASS J0130−4445A and L6±1 for 2MASS J0130−4445B.

We also derived classifications using a suite of spectral indices and spectral index/spectral type relations from Tokunaga & Kobayashi (1999), Reid et al. (2001), Geballe et al. (2002), Burgasser et al. (2006), and Burgasser (2007). Table 2 shows the measured values and the inferred spectral subtypes of 2MASS J0130−4445A and 2MASS J0130−4445B for each of the indices. The mean and scatter from these indices yields classifications of L0.5±1.0 for 2MASS J0130−4445A and L7.0±1.5 for 2MASS J0130−4445B. These are consistent with, but less precise than, the types inferred from spectral template matching, so we adopt the latter for our subsequent analysis.

4. SYSTEM PROPERTIES

4.1. *Is 2MASS J0130−4445 A Physical Binary?*

To assess whether two stars comprise a physical binary or are just a chance alignment of random stars, the most reliable method used is to check for a common systemic velocity. However, 2MASS J0130−4445B is very faint, even in the infrared, and has not been detected in any earlier epoch; hence, we do not have proper motions for the secondary nor radial velocities for either component. In the absence of kinematic information, we employed two other tests to examine whether

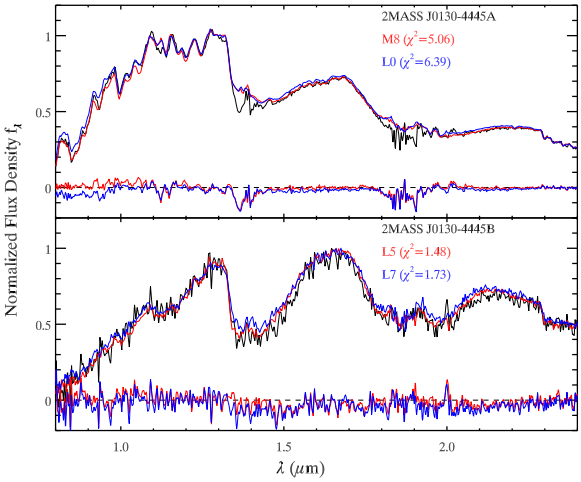

Figure 3. The spectral types for 2MASS J0130−4445AB as determined by matching their spectra with templates from the SpeX Prism Spectral Libraries. The best matches for 2MASS J0130−4445A were 2MASS J05173729−3348593 (optically classified M8; Cruz et al. 2003; Schmidt et al. 2007) and DENIS−P J0652197−253450 (optically classified L0; Phan-Bao et al. 2008) while 2MASSW J1326201−272937 (optically classified L5; Gizis 2002) and 2MASS J03185403−3421292 (optically classified L7; Kirkpatrick et al. 2008) were the best matches for 2MASS J0130−4445B. SpeX data for the templates are from Burgasser et al. (2010) and A. J. Burgasser et al. (in preparation). A χ^2 weighted mean of all the best fit templates gives spectral types of M9.0±0.5 and L6±1 for the two components, respectively. The residuals of the comparison (target − spectral type templates) are shown at the bottom of each panel.

Table 2
Near-Infrared Spectral Indices

Index	2MASS J0130−4445A		2MASS J0130−4445B		Reference
	Value	SpT	Value	SpT	
H_2O-J	0.954	L0.3	0.706	L7.1	1, 2
H_2O-H	0.876	M9.6	0.649	L8.3	1, 2
H_2O-A	0.686	L1.4	0.602	L4.1	3
H_2O-B	0.818	L0.3	0.517	L7.8	3
H_2O-1.5 μm[a]	1.216	M9.8	1.882	L9.0	4
CH_4-K	1.056	L2.1	0.968	L5.5	1, 2
CH_4-2.2 μm[b]	···	···	1.033	L5.7	4
K1[c]	0.069	M8.7	···	···	3, 5
Average SpT		L0.5±1.0		L7.0±1.5	

References. — (1) Burgasser et al. (2006); (2) Burgasser (2007); (3) Reid et al. (2001); (4) Geballe et al. (2002); (5) Tokunaga & Kobayashi (1999)

[a] The index H_2O-1.5 μm is well-defined only for spectral types L0 or later.
[b] The index CH_4-2.2 μm is well-defined only for spectral types L3 or later.
[c] The index K1 is well-defined only up to spectral type earlier than L6.

2MASS J0130−4445AB is a physical pair: (1) the heliocentric distances of the two components and (2) the probability that the sources are a chance alignment based on the surface distribution of stars on the sky.

The spectrophotometric distances to each component of 2MASS J0130−4445AB were derived using the M_J/spectral type relations from Cruz et al. (2003) based on the combined-light 2MASS photometry and our relative SpeX photometry (Table 3). The derived distances are 34.5±3.2 pc for the primary and 45.8±13.6 pc for the secondary, where the errors are from the uncertainties in the NIR spectral types (see Sec. 3.2). These distances are consistent with each other within their associated errors.

Table 3
Properties of 2MASS J01303563−4445411AB

Parameter	2MASS J0130-4445A	2MASS J0130-4445B	Reference
Optical Spectral Type	M9	···	1
NIR Spectral Type	M9.0±0.5	L6±1	2
J (mag)[a]	14.12±0.03	17.28±0.06	2,3
H (mag)[a]	13.48±0.03	16.13±0.10	2,3
K_s (mag)[a]	12.99±0.03	15.34±0.05	2,3
$J-K_s$ [a]	1.13±0.04	1.94±0.08	2,3
Est. $T_{\rm eff}$ (K)[b]	2400±110	1450±100	4
Est. Distance (pc) [c]	35±3	46±14	2,5
Projected Separation (AU) [d]	130±50		1,2
$V_{\rm tan}$ (km s^{-1})[d]	23±6		2,6

References. — (1) Reid et al. (2008); (2) This paper; (3) 2MASS (Cutri et al. 2003); (4) Stephens et al. (2009); (5) Cruz et al. (2003); (6) Faherty et al. (2009).

[a] Calculated using our relative magnitudes and the combined-light 2MASS photometry for the system.
[b] Reported uncertainties include scatter in the $T_{\rm eff}$/spectral type relation of Looper et al. (2008a) relation and uncertainties in the component classifications (±0.5 subtypes).
[c] Based on the M_J/spectral type relation of Cruz et al. (2003); uncertainties include photometric uncertainties and scatter in the Cruz et al. relation.
[d] Based on the average distance of 40±14 pc.

Next, we calculated the probability that 2MASS J0130−4445AB is a random chance alignment along our line-of-sight based on its three-dimensional position in the Galaxy. We followed Dhital et al. (2010), constructing a three-component Galactic model with the thin disk, thick disk, and halo, constrained with empirical stellar density profiles (Jurić et al. 2008; Bochanski et al. 2010). The model recreates a 30′×30′ region in the sky, centered around the coordinates of the given binary system, and out to heliocentric distances of 2500 pc. As all the simulated stars are single and non-associated, any visual binary is a random chance alignment. In 10^7 Monte Carlo realizations, we found, on average, 0.0285 chance alignments per realization on the sky, within the 3.″3 angular separation of 2MASS J0130−4445AB. More importantly, none of these chance alignments were within the range of spectrophotometric distances (40±14 pc) estimated for 2MASS J0130−4445AB. As such, we conservatively infer a $\lesssim 10^{-7}$ probability of positional coincidence. We therefore conclude that 2MASS J0130−4445AB is a physically-bound binary and not a chance alignment of two unassociated stars.

4.2. *Age & Mass Estimates for 2MASS J0130−4445AB*

The NIR spectral types of 2MASS J0130−4445A and 2MASS J0130−4445B correspond to effective temperatures, $T_{\rm eff}$, of 2400±110 K and 1450±100 K, respectively, based on the $T_{\rm eff}$/spectral type relation of Stephens et al. (2009). Uncertainties include scatter in the $T_{\rm eff}$ relation and uncertainties in the classifications (Sec. 3.2) added in quadrature. Figure 4 shows the Burrows et al. (1993, 1997) evolutionary models, displaying $T_{\rm eff}$ as a function of mass and age; the Burrows mass tracks and the observed $T_{\rm eff}$ ranges are shown as dotted and dashed lines and gray boxes, respectively. As the masses of the two components vary quite a bit with assumed age, it is imperative to constrain the age of 2MASS J0130−4445AB.

The absence of Li I in 2MASS J0130−4445A indicates that it is more massive than the predicted lithium depletion boundary (LDB) mass, ∼0.06 $M_\odot$ (Chabrier et al. 1996;

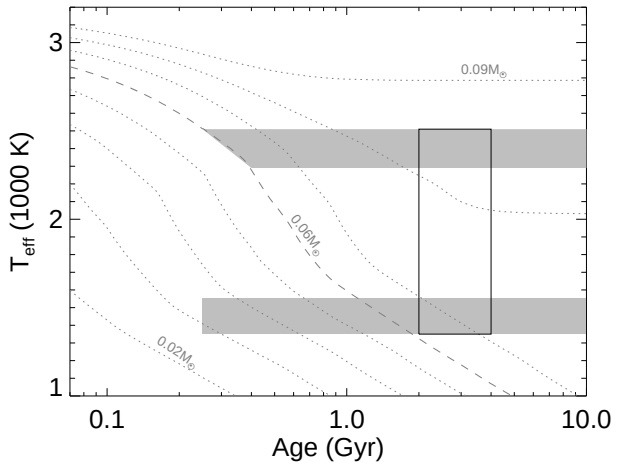

Figure 4. T_{eff} versus age for VLM stars and BDs based on the evolutionary models of Burrows et al. (1997). Tracks for masses of 0.02–0.09 $M_\odot$ in 0.01 $M_\odot$ steps are shown as dotted lines while the LDB limit of 0.06 $M_\odot$ is shown as a dashed line. The locus defined by this lower limit on age and T_{eff} derived from their spectral types is shown in gray for both components. The solid rectangle shows the age estimate of 2–4 Gyr based on the kinematics of Faherty et al. (2009). Note that the broad range of possible ages for this system allow a wide range of mass ratios, from 0.6 to 0.9.

Burrows et al. 2001) for field stars of solar metallicity. Using the T_{eff} for the primary based on its spectral type (including uncertainties) and assuming a mass $\gtrsim$0.06 $M_\odot$, the evolutionary models of Burrows et al. (1997) indicate an age $\gtrsim$250 Myr (Figure 4). We note that recent work by Baraffe & Chabrier (2010) has suggested that episodic accretion during the pre-main sequence stages causes central temperature of a star to increase up to 1 dex, with a sharp dependence on the frequency and magnitude of the episodic accretion. This serves to deplete Li I earlier than in non-accreting stars of the same mass and effectively reduces the inferred LDB mass and, thus, the minimum allowable age. Here, we have not taken episodic accretion into account. While we do not have an optical spectrum of the secondary, the presence (absence) of Li I in the spectrum would set a upper (lower) limit on the mass and, hence, the age of the system, in this case $\lesssim$1.8 Gyr ($\gtrsim$1.1 Gyr). The likely proximity of the mass of the secondary to the LDB is motivation to obtain an optical spectrum of this component.

The absence of Hα emission in the optical spectrum of 2MASS J0130−4445A and lack of UV or X-ray flux—the system is not detected in the GALEX (Martin et al. 2005) or the ROSAT (Voges et al. 1999) All-Sky Surveys—indicates that the system is not particularly active and, hence, not likely to be a very young system. This absence indicates that 2MASS J0130−4445AB is probably older than 1–100 Myr, as such emission has been detected in brown dwarfs in the Orion Nebula Cluster (isochronal age ∼1 Myr; Peterson et al. 2008), Taurus (∼3 Myr; Guieu et al. 2006), σ Orionis (2–7 Myr; Zapatero Osorio et al. 2002), α Persei (∼80 Myr; Stauffer et al. 1999), Pleiades (∼100 Myr; Stauffer et al. 1998; Martín et al. 2000), and Blanco 1 (∼100 Myr; P. A. Cargile et al., in prep.). However, activity signatures might not be reliable age indicators in the VLM regime. Both Hα and X-ray emission drop precipitously across the M dwarf/L dwarf transition (e.g., Kirkpatrick et al. 2000; Gizis et al. 2000; West et al. 2004; Stelzer et al. 2006), likely the result of reduced magnetic field coupling with increasingly neutral photospheres (e.g., Gelino et al. 2002; Mohanty et al. 2002).

Table 4
Model-dependent Properties of 2MASS J0130−4445AB
(Burrows et al. 1993, 1997)

Parameter	Age (Gyr)			
	0.25	2	4	10
Primary Mass ($M_\odot$)	0.055	0.082	0.083	0.083
Secondary Mass ($M_\odot$)	0.032	0.066	0.073	0.076
Mass Ratio	0.57	0.81	0.89	0.92
Log Binding Energy (erg)	41.61	41.96	41.97	41.97
Period (yr)	5030	3860	3760	3720

Extreme youth can also be ruled out based on the the NIR spectra of these sources, which do not exhibit the triangular H-band peaks seen in ∼100 Myr Pleiades M and L dwarfs (Bihain et al. 2010) and young field L dwarfs (e.g., Kirkpatrick et al. 2006). It is notable that 2MASS J0130−4445B is somewhat red compared to typical L6 dwarfs ($\langle J-K_s\rangle = 1.82\pm0.07$; Schmidt et al. 2010), as red sources have been shown to exhibit smaller velocity dispersions and, hence, younger ages (Faherty et al. 2009; Schmidt et al. 2010). However, 2MASS J0130−4445A is not unusually red for its spectral type ($\langle J-K_s\rangle = 1.12\pm0.10$); and the red color of the secondary may reflect an unusually dusty atmosphere (e.g., Looper et al. 2008b). Also, neither NIR spectra nor the optical spectrum of 2MASS J0130−4445A show high gravity signatures, i.e., unusually blue colors form enhanced H_2, or evidence of the system being metal-poor, making it unlikely that the system is as old as ∼10 Gyr (Burgasser et al. 2003a; Reid et al. 2007).

Considering the kinematics of the system, the tangential velocity of 2MASS J0130−4445A, 19±3 km s^{-1} is similar to the median velocities of the L dwarfs in the SDSS sample (28±25 km s^{-1}; Schmidt et al. 2010), the M9 dwarfs in the BDKP sample (23±23 km s^{-1}; Faherty et al. 2009), and the M7–L8 dwarfs in the 2MASS sample (25±21 km s^{-1}; Schmidt et al. 2007), with the quoted errors being the 1σ dispersions. The low tangential velocity suggests that 2MASS J0130−4445AB is part of the thin disk, although we note that we cannot rule out a higher space velocity for the binary system. Kinematic studies have found that late-M and L dwarfs with average kinematics are typically ∼2–4 Gyr old (Wielen 1977; Faherty et al. 2009).

In conclusion, based on the absence of Li I in the primary, we can place a (model-dependent) hard limit on the minimum age of 2MASS J0130−4445AB to be ∼250 Myr while its kinematics indicate a preferred age of ∼2–4 Gyr. Spectral features for both components are in agreement with these ages. For the ages of 0.25–10 Gyr, based on the Burrows et al. (1993) and Burrows et al. (1997) models, the estimated masses for 2MASS J0130−4445A and 2MASS J0130−4445B are 0.055–0.083 and 0.032–0.076 $M_\odot$, respectively, and the mass ratio is 0.57–0.92. For kinematics-based age limits of 2–4 Gyr, the estimated masses for 2MASS J0130−4445A and 2MASS J0130−4445B are 0.082–0.083 and 0.066–0.073 $M_\odot$, respectively, and the mass ratio is 0.81–0.89 (Table 4). Hence, the components straddle the hydrogen-burning mass limit; and this system is likely composed of a very low mass star and (massive) brown dwarf pair.

5. DISCUSSION

5.1. *Formation of Wide VLM Binaries in the Field*

With a projected separation of 130±50 AU, 2MASS J0130−4445AB is one of only ten VLM systems wider than 100 AU, with six of them in the field. All of these systems have been identified relatively recently; prior to their discovery, it was believed that VLM field systems were nearly all tight, a possible consequence of dynamic ejection early on. Based on this idea and the VLM binary population known at the time, two relations to define the largest possible separation of VLM binaries were proposed. First, Burgasser et al. (2003b) suggested that the maximum separation of a system was dependent on its mass: $a_{\max}$ (AU) $= 1400$ $(M_{tot}/M_{\odot})^2$. Second, Close et al. (2003) proposed that the stability of binary systems was contingent on their binding energy—a criterion based on the product rather than the sum of component masses; thus, only systems with binding energy $\geq 10^{42.5}$ erg would exist in the field[10]. For the (age-dependent) estimated mass of 2MASS J0130−4445AB, the Burgasser et al. (2003b) relation equates to maximum physical separations of only 9.2 AU and 35.4 AU for ages of 0.25 and 10 Gyr, respectively, which are both much smaller than the physical separation we have measured for 2MASS J0130−4445AB. Similarly, the binding energies for the system are $10^{41.61}$ and $10^{41.97}$ erg for the same ages (see Table 4). Both the Burgasser et al. (2003b) and Close et al. (2003) relations are definitively violated by 2MASS J0130−4445AB, for all ages and mass ratios. Assuming these limits emerge from dynamical scattering processes, this binary seems unlikely to have formed via the ejection of protostellar embryos.

More recently, Zuckerman & Song (2009) have argued that fragmentation, rather than dynamical, processes are more likely to describe the boundary for the lowest binding energy systems. A protostellar cloud can only fragment if it is more massive than the minimum Jeans mass ($\sim$7 M_J; Low & Lynden-Bell 1976). Assuming fiducial separations of 300 AU for the fragments, they derived a cut-off for binding energy as a function of total systemic mass. Finding that this disfavors the formation of very wide and/or high mass ratio binaries, Faherty et al. (2010) used the Jeans length, instead of the fiducial separation, and mass ratio of the system. For 2MASS J0130−4445AB at 0.25 Gyr ($M_{tot}\approx$0.1 $M_{\odot}$), Zuckerman & Song (2009) and Faherty et al. (2010) relations suggest minimum binding energies of $10^{40.5}$ and 10^{39} erg, respectively; if the system were older, they would be even more stable due to the higher masses. 2MASS J0130−4445AB is well within the bounds of both Zuckerman & Song (2009) and Faherty et al. (2010) formation criteria for all ages and mass ratios. Hence, the observed wide, low binding energy VLM binaries could have formed from small protostellar clouds, with masess close to the local Jeans mass.

Current numerical simulations have suggested an alternative mechanism to form wide binaries: N-body dynamics in small clusters disrupt the VLM pairs wider than $\sim$60 AU, and very wide systems ($> 10^4 - 10^5$ AU) can then be formed when stars are ejected into the field in the same direction (Moeckel & Bate 2010; Kouwenhoven et al. 2010). While this provides a mechanism to create the most fragile VLM pairs identified to date, it does not aid in the formation of 100–1000 AU pairs like 2MASS J0130−4445AB. Two other VLM systems in this separation range are known: 2MASSJ 1623361−240221 (220 AU; Billères et al. 2005) and SDSS J141623.94+134826.3 (100 AU; Burningham et al. 2010; Scholz 2010).

[10] We note that for the small separations and a mass ratio highly skewed toward one, which was the case for the VLM binaries known at the time, the Burgasser et al. (2003b) and Close et al. (2003) limits are essentially equivalent.

5.2. *2MASS J0130−4445AB as a Probe of the M Dwarf/L Dwarf Transition*

The components of 2MASS J0130−4445AB straddle a spectral type range that is particularly interesting for three reasons. First, condensate clouds become an important source of photospheric opacity and thermal evolution starting at the end of the M dwarf sequence and peaking in influence in the middle of the L dwarf sequence (Ackerman & Marley 2001; Kirkpatrick et al. 2008; Saumon & Marley 2008). With a component on either end of this regime, 2MASS J0130−4445AB is a particularly useful coeval laboratory for studying the emergence and dispersal of these clouds. Second, both components straddle the hydrogen-burning mass limit; and the secondary is very near the LDB. Detection of Li I in the optical spectrum of the secondary could provide a relatively precise constraint on the age of this system (0.25–1.8 Gyr) and thereby make it a useful benchmark for studies of brown dwarf thermal evolution and atmospheric models (e.g., Pinfield et al. 2006). Third, the M dwarf/L dwarf transition exhibits a steep decline in magnetic activity metrics, including Hα, UV, and X-ray emission (e.g., Gizis et al. 2000; West et al. 2004) but notably not radio emission (e.g., Berger 2006; Berger et al. 2010). This is believed to be due to the decoupling of magnetic fields from an increasingly neutral photosphere (Gelino et al. 2002; Mohanty et al. 2002) but does not rule out the presence of significant magnetic fields (Reiners & Basri 2007). While Hα is absent in the spectrum of 2MASS J0130−4445A, examination of field strengths and radio emission in this coeval pair may facilitate understanding of how magnetic fields evolve across the stellar/brown dwarf transition. As one of only three binaries spanning the M dwarf/L dwarf transition whose components are easily resolvable from ground-based facilities (the other two are the 1.″2 L1.5+L4.5 2MASSJ 1520022−442242 and the 1.″0 M9+L3 2MASSJ 1707234−055824; Burgasser 2004; Burgasser et al. 2007a; Folkes et al. 2007), 2MASS J0130−4445AB is an important laboratory for studying how condensate clouds, lithium burning, and magnetic activity trends vary across this transition.

6. SUMMARY

We have identified a binary companion to 2MASS J01303563−4445411A based on NIR imaging and spectroscopic observations. The secondary is well-separated ($\Delta\theta = 3.''2$) and much fainter ($\Delta K \approx 2.35$ mags). Based on template matching and spectral indices, we have calculated the NIR spectral types to be M9.0±0.5 and L6±1 for the two components. The optical spectrum of 2MASS J0130−4445A shows no evidence of either Hα or Li I indicating a minimum age of 0.25 Gyr, while the kinematics suggest an age of 2–4 Gyr. However, we would like to stress that 0.25–10 Gyr, with the lower bound set by LDB and activity, is the more secure age for the system. 2MASS J0130−4445AB is likely a "grown-up" wide binary that has survived ejections and/or dynamical interactions. More importantly, the system definitively violates the binary stability limits based on the ejection hypothesis (Burgasser et al. 2003b; Close et al.

2003) and satisfies the limits based on the idea that wide VLM binaries are formed from approximately Jeans mass-sized protostellar clouds (Zuckerman & Song 2009; Faherty et al. 2010). This suggests that observed wide VLM binaries may have formed differently than single VLMs and/or tighter binaries. As one of ten VLM systems with separations $\gtrsim$100 AU, 2MASS J0130−4445AB provides a stringent test for theoretical studies of VLM binary formation, as well as a well-resolved, coeval laboratory for studying empirical trends across the M dwarf/L dwarf and stellar/brown dwarf transitions.

The authors would like to thank the anonymous referee for his/her comments on the manuscript, telescope operator Paul Sears and instrument specialist John Rayner for their assistance during the IRTF observations, and Kelle Cruz for providing an electronic version of the optical spectrum of 2MASS J0130−4445A. SD and KGS acknowledge funding support through NSF grant AST-0909463. This publication makes use of data from the Two Micron All Sky Survey, which is a joint project of the University of Massachusetts and the Infrared Processing and Analysis Center, and funded by the National Aeronautics and Space Administration and the National Science Foundation. 2MASS data were obtained from the NASA/IPAC Infrared Science Archive, which is operated by the Jet Propulsion Laboratory, California Institute of Technology, under contract with the National Aeronautics and Space Administration. This research has made use of the VLM Binaries Archive, maintained by Nick Siegler at `http://www.vlmbinaries.org`; the SpeX Prism Spectral Libraries, maintained by Adam Burgasser at `http://www.browndwarfs.org/spexprism`; and the M, L, and T dwarf compendium housed at DwarfArchives.org and maintained by Chris Gelino, Davy Kirkpatrick, and Adam Burgasser. The authors wish to recognize and acknowledge the very significant cultural role and reverence that the summit of Mauna Kea has always had within the indigenous Hawaiian community. We are most fortunate to have the opportunity to conduct observations from this mountain.

Facilities: IRTF (SpeX)

REFERENCES

Ackerman, A. S., & Marley, M. S. 2001, ApJ, 556, 872
Baraffe, I., & Chabrier, G. 2010, å
Basri, G., & Reiners, A. 2006, AJ, 132, 663
Bate, M. R. 2009, MNRAS, 392, 590
Berger, E. 2006, ApJ, 648, 629
Berger, E., et al. 2010, ApJ, 709, 332
Bihain, G., Rebolo, R., Zapatero Osorio, M. R., Béjar, V. J. S., & Caballero, J. A. 2010, A&A, 519, A93+
Billères, M., Delfosse, X., Beuzit, J., Forveille, T., Marchal, L., & Martín, E. L. 2005, A&A, 440, L55
Bochanski, J. J., Hawley, S. L., Covey, K. R., West, A. A., Reid, I. N., Golimowski, D. A., & Ivezić, Ž. 2010, AJ, 139, 2679
Burgasser, A. J. 2004, ApJS, 155, 191
——. 2007, ApJ, 659, 655
Burgasser, A. J., Cruz, K. L., Cushing, M., Gelino, C. R., Looper, D. L., Faherty, J. K., Kirkpatrick, J. D., & Reid, I. N. 2010, ApJ, 710, 1142
Burgasser, A. J., Cruz, K. L., & Kirkpatrick, J. D. 2007a, ApJ, 657, 494
Burgasser, A. J., Geballe, T. R., Leggett, S. K., Kirkpatrick, J. D., & Golimowski, D. A. 2006, ApJ, 637, 1067
Burgasser, A. J., et al. 2003a, ApJ, 592, 1186
Burgasser, A. J., Kirkpatrick, J. D., Reid, I. N., Brown, M. E., Miskey, C. L., & Gizis, J. E. 2003b, ApJ, 586, 512
Burgasser, A. J., Liu, M. C., Ireland, M. J., Cruz, K. L., & Dupuy, T. J. 2008, ApJ, 681, 579
Burgasser, A. J., Looper, D. L., Kirkpatrick, J. D., & Liu, M. C. 2007b, ApJ, 658, 557
Burgasser, A. J., Reid, I. N., Siegler, N., Close, L., Allen, P., Lowrance, P., & Gizis, J. 2007c, in Protostars and Planets V, ed. B. Reipurth, D. Jewitt, & K. Keil (Tucson, AZ: Univ. Arizona Press), 427
Burningham, B., et al. 2010, MNRAS, 404, 1952
Burrows, A., Hubbard, W. B., Lunine, J. I., & Liebert, J. 2001, Reviews of Modern Physics, 73, 719
Burrows, A., Hubbard, W. B., Saumon, D., & Lunine, J. I. 1993, ApJ, 406, 158
Burrows, A., et al. 1997, ApJ, 491, 856
Caselli, P., Benson, P. J., Myers, P. C., & Tafalla, M. 2002, ApJ, 572, 238
Chabrier, G., Baraffe, I., & Plez, B. 1996, ApJ, 459, 91
Close, L. M., Siegler, N., Freed, M., & Biller, B. 2003, ApJ, 587, 407
Cruz, K. L., Reid, I. N., Liebert, J., Kirkpatrick, J. D., & Lowrance, P. J. 2003, AJ, 126, 2421
Cushing, M. C., et al. 2008, ApJ, 678, 1372
Cushing, M. C., Rayner, J. T., & Vacca, W. D. 2005, ApJ, 623, 1115
Cushing, M. C., Vacca, W. D., & Rayner, J. T. 2004, PASP, 116, 362
Cutri, R. M., et al. 2003, 2MASS All Sky Catalog of Point Sources. (The IRSA 2MASS All-Sky Point Source Catalog, NASA/IPAC Infrared Science Archive. http://irsa.ipac.caltech.edu/applications/Gator/)
Dhital, S., West, A. A., Stassun, K. G., & Bochanski, J. J. 2010, AJ, 139, 2566
Duquennoy, A., & Mayor, M. 1991, A&A, 248, 485
Faherty, J. K., Burgasser, A. J., Cruz, K. L., Shara, M. M., Walter, F. M., & Gelino, C. R. 2009, AJ, 137, 1
Faherty, J. K., Burgasser, A. J., West, A. A., Bochanski, J. J., Cruz, K. L., Shara, M. M., & Walter, F. M. 2010, AJ, 139, 176
Fischer, D. A., & Marcy, G. W. 1992, ApJ, 396, 178
Folkes, S. L., Pinfield, D. J., Kendall, T. R., & Jones, H. R. A. 2007, MNRAS, 378, 901
Geballe, T. R., et al. 2002, ApJ, 564, 466
Gelino, C. R., Marley, M. S., Holtzman, J. A., Ackerman, A. S., & Lodders, K. 2002, ApJ, 577, 433
Gizis, J. E. 2002, ApJ, 575, 484
Gizis, J. E., Monet, D. G., Reid, I. N., Kirkpatrick, J. D., Liebert, J., & Williams, R. J. 2000, AJ, 120, 1085
Goodwin, S. P., Whitworth, A. P., & Ward-Thompson, D. 2004a, A&A, 414, 633
——. 2004b, A&A, 423, 169
Guieu, S., Dougados, C., Monin, J., Magnier, E., & Martín, E. L. 2006, A&A, 446, 485
Joergens, V. 2008, A&A, 492, 545
Jurić, M., et al. 2008, ApJ, 673, 864
Kirkpatrick, J. D. 2005, ARA&A, 43, 195
Kirkpatrick, J. D., Barman, T. S., Burgasser, A. J., McGovern, M. R., McLean, I. S., Tinney, C. G., & Lowrance, P. J. 2006, ApJ, 639, 1120
Kirkpatrick, J. D., et al. 2008, ApJ, 689, 1295
——. 1999, ApJ, 519, 802
——. 2000, AJ, 120, 447
Kouwenhoven, M. B. N., Goodwin, S. P., Parker, R. J., Davies, M. B., Malmberg, D., & Kroupa, P. 2010, MNRAS, 404, 1835
Kroupa, P. 1995, MNRAS, 277, 1491
Lépine, S., & Bongiorno, B. 2007, AJ, 133, 889
Looper, D. L., Gelino, C. R., Burgasser, A. J., & Kirkpatrick, J. D. 2008a, ApJ, 685, 1183
Looper, D. L., et al. 2008b, ApJ, 686, 528
Low, C., & Lynden-Bell, D. 1976, MNRAS, 176, 367
Martin, D. C., et al. 2005, ApJ, 619, L1
Martín, E. L., Brandner, W., Bouvier, J., Luhman, K. L., Stauffer, J., Basri, G., Zapatero Osorio, M. R., & Barrado y Navascués, D. 2000, ApJ, 543, 299
McElwain, M. W., & Burgasser, A. J. 2006, AJ, 132, 2074
McLean, I. S., McGovern, M. R., Burgasser, A. J., Kirkpatrick, J. D., Prato, L., & Kim, S. S. 2003, ApJ, 596, 561
Moeckel, N., & Bate, M. R. 2010, MNRAS, 404, 721
Mohanty, S., Basri, G., Shu, F., Allard, F., & Chabrier, G. 2002, ApJ, 571, 469
Peterson, D. E., et al. 2008, ApJ, 685, 313
Phan-Bao, N., et al. 2008, MNRAS, 383, 831
Pinfield, D. J., Jones, H. R. A., Lucas, P. W., Kendall, T. R., Folkes, S. L., Day-Jones, A. C., Chappelle, R. J., & Steele, I. A. 2006, MNRAS, 368, 1281

Rayner, J. T., Toomey, D. W., Onaka, P. M., Denault, A. J., Stahlberger, W. E., Vacca, W. D., Cushing, M. C., & Wang, S. 2003, PASP, 115, 362
Reid, I. N., Burgasser, A. J., Cruz, K. L., Kirkpatrick, J. D., & Gizis, J. E. 2001, AJ, 121, 1710
Reid, I. N., Cruz, K. L., Kirkpatrick, J. D., Allen, P. R., Mungall, F., Liebert, J., Lowrance, P., & Sweet, A. 2008, AJ, 136, 1290
Reid, I. N., & Gizis, J. E. 1997, AJ, 113, 2246
Reid, I. N., Turner, E. L., Turnbull, M. C., Mountain, M., & Valenti, J. A. 2007, ApJ, 665, 767
Reiners, A., & Basri, G. 2007, ApJ, 656, 1121
Reipurth, B., & Clarke, C. 2001, AJ, 122, 432
Saumon, D., & Marley, M. S. 2008, ApJ, 689, 1327
Schmidt, S. J., Cruz, K. L., Bongiorno, B. J., Liebert, J., & Reid, I. N. 2007, AJ, 133, 2258
Schmidt, S. J., West, A. A., Hawley, S. L., & Pineda, J. S. 2010, AJ, 139, 1808
Scholz, R. 2010, A&A, 510, L8+
Simons, D. A., & Tokunaga, A. 2002, PASP, 114, 169
Skrutskie, M. F., et al. 2006, AJ, 131, 1163
Stauffer, J. R., et al. 1999, ApJ, 527, 219
Stauffer, J. R., Schultz, G., & Kirkpatrick, J. D. 1998, ApJ, 499, L199+
Stelzer, B., Micela, G., Flaccomio, E., Neuhäuser, R., & Jayawardhana, R. 2006, A&A, 448, 293
Stephens, D. C., et al. 2009, ApJ, 702, 154
Tokunaga, A. T., & Kobayashi, N. 1999, AJ, 117, 1010
Tokunaga, A. T., Simons, D. A., & Vacca, W. D. 2002, PASP, 114, 180
Tsuji, T., Ohnaka, K., Aoki, W., & Jones, H. R. A. 1998, Highlights of Astronomy, 11, 439
Vacca, W. D., Cushing, M. C., & Rayner, J. T. 2003, PASP, 115, 389
Voges, W., et al. 1999, VizieR Online Data Catalog, 9010, 0
Watkins, S. J., Bhattal, A. S., Boffin, H. M. J., Francis, N., & Whitworth, A. P. 1998a, MNRAS, 300, 1205
——. 1998b, MNRAS, 300, 1214
West, A. A., et al. 2004, AJ, 128, 426
Whitworth, A. P., & Zinnecker, H. 2004, A&A, 427, 299
Wielen, R. 1977, A&A, 60, 263
Zapatero Osorio, M. R., Béjar, V. J. S., Pavlenko, Y., Rebolo, R., Allende Prieto, C., Martín, E. L., & García López, R. J. 2002, A&A, 384, 937
Zuckerman, B., & Song, I. 2009, A&A, 493, 1149